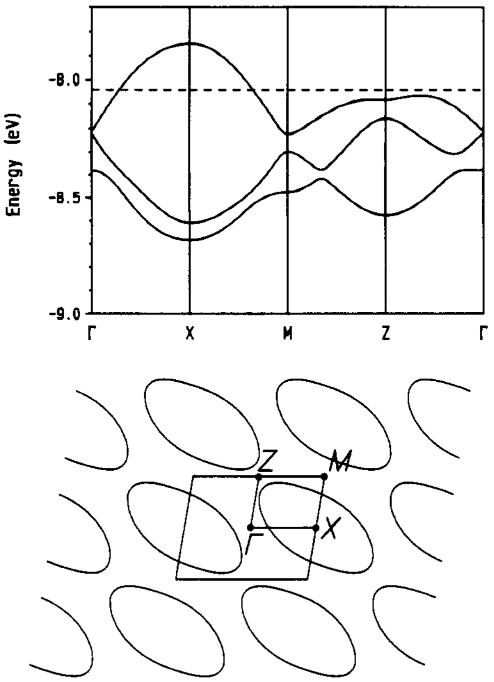

Figure 3. (a, top) Dispersion relations of the highest three occupied bands calculated for a donor-molecule layer of $\beta_{\rm m}$-(BEDO-TTF)$_3$Cu$_2$(NCS)$_3$. The dashed line refers to the Fermi level; $\Gamma = (0, 0)$, $X = (a^*/2, 0)$, $Z = (0, c^*/2)$, and $M = (a^*/2, c^*/2)$. (b, bottom) Fermi surface associated with the highest occupied band of $\beta_{\rm m}$-(BEDO-TTF)$_3$Cu$_2$(NCS)$_3$ in an extended zone scheme, where the parallelogram represents a primitive cell in reciprocal space.

is also the case for $\beta_{\rm m}$-(BEDO-TTF)$_3$Cu$_2$(NCS)$_3$, then crystals varying from single domain to those with a high density of stacking faults would produce varying intensities for the (h, k, $l \pm {}^1/_3$) satellite reflections.

Superconducting Transition. Superconductivity in the crystals was detected by use of rf penetration depth measurements[13] carried out to temperatures as low as 0.58 K. In this method, superconductivity is detected by an increase in the resonant frequency ($\sim$580 kHz) of an rf coil in an inductance–capacitance circuit caused by the exclusion of the field in the test sample due to the occurrence of diamagnetic shielding currents. This is an ac shielding experiment and not a Meissner effect measurement, but the increasing resonant frequency relative to that of the empty coil is an approximate measure of the ac susceptibility and, therefore, indicates the existence of volume superconductivity. A plot of the resonant frequency versus temperature is illustrated in Figure 2. This figure shows a change in the resonant frequency of $\sim$2.7 kHz below $\sim$1 K for a sample of mass $\sim$750 μg. The large change in frequency relative to the mass indicates that the sample itself rather than some minor impurity is the source of the superconducting signal. The tail of the superconducting transition begins near 1.2 K, but an extrapolation of the nearly linear portion of the transition curve gives $T_c = 1.06 \pm 0.02$ K for the onset temperature of the bulk of the sample.

Band Electronic Structure. The electronic structure of $\beta_{\rm m}$-(BEDO-TTF)$_3$Cu$_2$(NCS)$_3$ was examined by performing tight-binding band calculations[14] on its donor-molecule layer. Figure 3a shows the dispersion relations of the three highest occupied bands, which are largely represented by the HOMO of BEDO-TTF. As in the case of BEDT-TTF, the HOMO of BEDO-TTF is mainly concentrated on the central TTF moiety. The donor-molecule layer of $\beta_{\rm m}$-(BEDT-TTF)$_3$Cu$_2$(NCS)$_3$ has three molecules per unit cell. With the formal oxidation (BEDO-TTF)$_3{}^+$, therefore, the highest occupied band of Figure 3a is half-filled. The Fermi surface associated with this band is shown in Figure 3b, which consists of ellipse-like hole pockets centered at X and its equivalent points. Thus $\beta_{\rm m}$-(BEDO-TTF)$_3$Cu$_2$(NCS)$_3$ is predicted to be a two-dimensional metal. Although $\beta_{\rm m}$-(BEDO-TTF)$_3$Cu$_2$(NCS)$_3$ is a 3:1 salt, its electronic structure has a characteristic feature found in almost all superconducting 2:1 salts, viz., a half-filled band leading to a closed Fermi surface.[1a] The donor-layer packing pattern of this salt is quite similar to that of (BEDO-TTF)$_2$X (X$^-$ = AuBr$_2^-$, ClO$_4^-$).[7] The donor molecules make short C–H···O contacts not only within each donor stack, but also between adjacent donor stacks. Due to slight differences in the interstack donor-donor overlap, $\beta_{\rm m}$-(BEDO-TTF)$_3$Cu$_2$(NCS)$_3$ has a two-dimensional Fermi surface, but the (BEDO-TTF)$_2$X (X$^-$ = AuBr$_2^-$ ClO$_4^-$) salts have one-dimensional Fermi surfaces.[7]

In summary, we have found the first organic superconductor based on an oxygen-containing donor molecule. This result opens up a completely new avenue in the search for organic superconductors with ever increasing transition temperatures.

Acknowledgment. Work at Argonne National Laboratory and at North Carolina State University was supported by the Office of Basic Energy Sciences, Division of Materials Sciences, U.S. Department of Energy, under Contract W-31-109-ENG-38 and Grant DE-FG05-86ER45259, respectively. We thank E. Huff for the ICP Cu analysis. J.E.T. is a student research participant sponsored by the Argonne Division of Educational Programs from the University of Michigan (Ann Arbor, MI).

Supplementary Material Available: Tables of crystal structure data collection and refinement parameters (Table S1) and final atom positional parameters (Table S2) for $\beta_{\rm m}$-(BEDO-TTF)$_3$Cu$_2$(NCS)$_3$ (3 pages). Ordering information is given on any current masthead page.

---

(12) Ravy, S.; Pouget, J. P.; Lenoir, C.; Batail, P. *Solid State Commun.* **1990**, *73*, 37.

(13) Crabtree, G. W.; Carlson, K. D.; Hall, L. N.; Copps, P. T.; Wang, H. H.; Emge, T. J.; Beno, M. A.; Williams, J. M. *Phys. Rev. B: Condens. Matter* **1984**, *30*, 2958.

(14) Details of our tight-binding band electronic structure calculations, based upon the extended Hückel method,[15] are described elsewhere.[16,17]

(15) Hoffmann, R. *J. Chem. Phys.* **1963**, *39*, 1397.

(16) Whangbo, M.-H.; Hoffman, R. *J. Am. Chem. Soc.* **1978**, *100*, 6093.

(17) The valence atomic orbitals of C, O, and S are represented by double-ζ Slater-type functions. For details of the atomic parameters employed for our calculations, see ref 7.

(18) Bardeen, J.; Cooper, L. N.; Schrieffer, J. R. *Phys. Rev.* **1957**, *106*, 162; **1957**, *108*, 1175.

Chemistry and Materials Science Divisions
Argonne National Laboratory
Argonne, Illinois 60439

Mark A. Beno*
Hau H. Wang*
Aravinda M. Kini
K. Douglas Carlson*
Urs Geiser*
W. K. Kwok
James E. Thompson
Jack M. Williams*

Department of Chemistry
North Carolina State University
Raleigh, North Carolina 27695-8204

Jingqing Ren
Myung-Hwan Whangbo*

Received March 14, 1990

Synthesis and Structural Characterization of [*cis*-(Cy$_2$PCH$_2$CH$_2$PCy$_2$)(*neo*-Pe)PtGa(*neo*-Pe)$_2$] (Cy = c-C$_6$H$_{11}$; *neo*-Pe = CH$_2$C(CH$_3$)$_3$)

We have been interested in the synthesis of organotransition-metal–group III[1] complexes to serve as precursors for the deposition of intermetallic films[2] of specified composition using organometallic chemical vapor deposition (OMCVD).[3] Mixed-metal complexes such as dichloro(tetracarbonylcobalt)gallium(III) tetrahydrofuranate[4] or platinumbis(dimethylglyoximato)bis(dimethylgallium)[5] have given depositions of CoGa or PtGa$_2$[6] that are crystalline and highly reflective. However, these contain trace contaminations of heteroatoms derived from the ligands. On the

---

(1) Group 13 according to the recent IUPAC recommendation.

(2) (a) Lince, J. R.; Tsai, C. T.; Williams, R. S. *J. Mater. Res.* **1986**, *1*, 537. (b) Kim, Y. K.; Shuh, D. K.; Williams, R. S.; Sadwick, L. P.; Wang, K. L. *Proc. Mater. Res. Soc.* **1989**, *148*, 15.

(3) Yablonovitch, E. *Science* **1989**, *246*, 347.

way to synthesize other mixed metal complexes we examined the interaction of organogallium compounds with platinum derivatives that were known to give rise to reactive, coordinatively unsaturated fragments.[7,8]

With *cis*-$(Et_3P)_2PtH_2$[7] and GaR_3 derivatives (R = CH_3, $CH{=}CH_2$, C_6H_5) we obtained spectroscopic evidence for reactions in the range −78 to 0 °C; however, the mixtures were complex and not amenable to separation. When [*cis*-$(CyPH_2CH_2PCy_2)Pt$(*neo*-Pe)H] (**1**)[8] is treated with excess trimethylgallium at 26 °C, over a period of several days we observe gas evolution and nearly complete alkyl exchange and methyl transfer to yield the dimethyl analogue of **1**, among other products.[9] We were thus led to combine **1** with excess Ga(*neo*-Pe)$_3$ as shown in eq 1.

$$\underset{\mathbf{1}}{[\textit{cis}\text{-}(Cy_2PCH_2CH_2PCy_2)Pt(\textit{neo}\text{-}Pe)(H)]} + Ga(\textit{neo}\text{-}Pe)_3 \xrightarrow[90\ ^\circ C]{CH_3C_6H_{11}} \underset{\mathbf{2}}{[\textit{cis}\text{-}(Cy_2PCH_2CH_2PCy_2)(\textit{neo}\text{-}Pe)PtGa(\textit{neo}\text{-}Pe)_2]} + C(CH_3)_4 \quad (1)$$

$$Cy = c\text{-}C_6H_{11};\ \textit{neo}\text{-}Pe = CH_2C(CH_3)_3$$

A quantity of **1** (250 mg, 0.28 mmol) is treated with a 5-fold excess of trineopentylgallium[10] (ca. 0.5 mL) together with 2 mL of methylcyclohexane in a 100-mL Schlenk flask equipped with a vacuum stopcock adapter. The contents are cooled to −78 °C, and the flask is evacuated. After warm up, it is heated to 90 °C for 3 h. Evolution of gas is observed as the solution nears 90 °C, while an initial white suspension becomes a deep yellow solution. After the gas evolution is complete, the reaction mixture is allowed to stand at 90 °C for 1 h. The mixture is then allowed to cool, and all volatile constituents are removed under vacuum (10^{-3} Torr) at 50 °C over a period of 3 days. An initial oily product crystallizes. The crystals are then washed three times with 0.5 mL of dry pentane at −80 °C and then dried again in high vacuo at 50 °C. Yield: 311 mg (96%) of analytically pure **2**.[11]

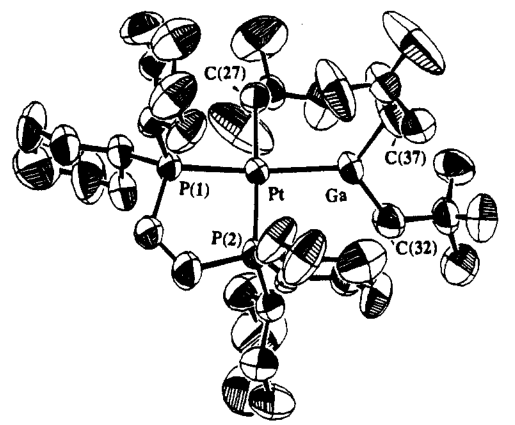

Figure 1. ORTEP projection of [*cis*-$(Cy_2PCH_2CH_2PCy_2)$(*neo*-Pe)PtGa(*neo*-Pe)$_2$] (**2**) with hydrogen atoms omitted for clarity. Thermal ellipsoids represent 50% probability. Selected bond distances (pm): Pt–Ga, 243.8 (1); Pt–C(27), 213 (1); Ga–C(37), 200 (1); Ga–C(32), 202 (1); Pt–P(1), 231.7 (3); Pt–P(2), 225.2 (4). Selected angles (deg): C(27)–Pt–Ga, 86.9; P(2)–Pt–Ga, 95.7; P(2)–Pt–P(1), 86.1; P(1)–Pt–C(27), 92.3.

X-ray analysis was undertaken,[12] and the ORTEP is shown in Figure 1. The compound exhibits a Pt–Ga separation that is *shorter* than the sum of the covalent single-bond radii (259[13a] or 265[13b] pm). The coordination geometry at the gallium site in **2** is trigonal planar; no interaction is indicated with adjacent atoms, i.e. Ga–C(27) = 315 pm and Ga–P(2) = 348 pm. We propose back-donation via d_π–p_π interactions[14] to be responsible for the Pt–Ga bond shortening. It is interesting to note in this connection that the dihedral angle between the planes defined by Pt–P(1)–P(2) and Ga–C(32)–C(37) is 123.1°. There are few structural data on compounds with a direct gallium to transition-metal bond, the closest one (containing an R_2Ga group) being [(η^5-C_5H_5)$(CO)_3WGa(CH_3)_2$], with W–Ga = 270.8 pm.[15] By contrast to the present case, this distance is somewhat *longer* than estimated from covalent single-bond radii (261[13a] or 265[13b] pm).

The coordination around the platinum atom in **2** can be described as distorted square planar. The Pt–P(1) and Pt–P(2) distances differ by 6.5 pm (see Figure 1), and two different phosphorus resonances are observed.[11] This effect reflects the difference in trans influence of the gallium dialkyl as compared to the alkyl ligand. There is great steric hindrance around the Pt–Ga bond, which may contribute to the stability (and isolability) of the compound. For example, no THF adduct is seen to form, as monitored by ^1H and ^{31}P NMR spectroscopy (C_6H_6 solution, 25 °C), similar to what is reported for trineopentylgallium.[10] Also, hydrolysis in aqueous THF is slow, occurring over several days (reaction products not yet identified). The compound exhibits very low volatility, no material subliming up to 130 °C at 10^{-3} Torr, at which point melting and onset of thermal decomposition are observed.

Acknowledgment. Dr. H.-J. Müller was supported by a stipend from the NATO Science Committee in cooperation with the Deutscher Akademischer Austausch Dienst. Dr. R. A. Fischer was supported by the Feodor Lynen Fund of the Alexander von Humboldt Foundation (FRG) supplemented by a grant from SDIO/IST managed by the Office of Naval Research.

Supplementary Material Available: Text describing details of data collection, reduction, and refinement, a full table of crystal and refinement data, and tables of atom positions and equivalent isotropic temperature factors, calculated hydrogen atom positions, anisotropic temperature factors, and interatomic distances and angles (9 pages); a listing of observed and calculated structure factors (21 pages). Ordering information is given on any current masthead page.

Department of Chemistry & Biochemistry
University of California
Los Angeles, California 90024-1569

R. A. Fischer
H. D. Kaesz*
S. I. Khan
H.-J. Müller

Received January 16, 1990

---

(4) Patmore, D. J.; Graham, W. A. G. *Inorg. Chem.* **1966**, *5*, 1586.

(5) Kohler, U.; Hansen, H. D.; Weidlein, J. *J. Organomet. Chem.* **1984**, *272*, 337.

(6) Chen, Y.-J.; Kaesz, H. D.; Kim, Y. K.; Müller, H.-J.; Williams, R. S.; Xue, Z. *Appl. Phys. Lett.* **1989**, *55*, 2760.

(7) Paonessa, R. S.; Trogler, W. C. *Organometallics* **1982**, *1*, 768.

(8) Hackett, M.; Whitesides, G. M. *J. Am. Chem. Soc.* **1988**, *110*, 1449.

(9) The complex *cis*-$[(Cy_2PCH_2CH_2PCy_2)Pt(CH_3)_2$ was identified by ^1H and ^{31}P NMR spectroscopy with an authentic sample independently synthesized by treating *cis*-$(C_8H_{12})PtCl_2$ with $Cy_2PCH_2CH_2PCy_2$, followed by treatment of the resulting *cis*-$[(Cy_2PCH_2CH_2PCy_2)PtCl_2$ with MeLi.

(10) (a) Beachley, O. T., Jr.; Pazik, J. C. *Organometallics* **1988**, *7*, 1516. (b) A 5-fold excess of the reagent is required to minimize side reactions.

(11) Anal. for $C_{41}H_{81}GaP_2Pt$ (**2**). Calcd: C, 54.67; H, 9.06. Found (Galbraith Analytical Laboratories, Knoxville, TN): C, 54.37; H, 9.21. ^1H NMR (360 MHz, C_6D_6, 25 °C, δ in ppm, relative to TMS): 2.54 (dd, 2 H; $^2J(Pt–H)$ = 31.5 Hz; $^3J(P–H)$ = 13.1 and 6.1), 2.3–1.16 (broad signal groups, 50 H), 1.47 (s, 18 H), 1.38 (s, 9 H). $^{13}C\{^1H\}$ NMR (90.56 MHz, C_6D_6, 25 °C, δ in ppm, relative to external TMS): 50.36 (d, $^2J(P_{trans}–C)$ = 22.3 Hz; $^1J(Pt–C)$ = 128.6 Hz), 35.2 (s), 34.7 (s), 36.6–22.4 (complex multiplets). ^{31}P NMR (145.78 MHz, C_6D_6, 25 °C, δ in ppm, relative to 85% phosphoric acid): 70.65 (d, $^2J(P–P)$ = 2.0 Hz; $^1J(Pt–P)$ = 1895 Hz), 66.14 (d, $^2J(P–P)$ = 2.0 Hz; $^1J(Pt–P)$ = 1339 Hz).

(12) Several crystals of **2** were selected and each placed into a Lindemann tube in a drybox. The tubes were sealed under argon and were examined by microscope. Suitable looking specimens were mounted on a four-circle automated diffractometer. X-ray analysis: Formula, $PtGaP_2C_{41}H_{81}$; fw 900.85; monoclinic, $P2_1/c$, a = 17.896 (1) Å, b = 11.249 (1) Å, c = 22.887 (1) Å, β = 98.48 (1)°, Z = 4; V = 4557.06 Å^3, ρ_{calcd} = 1.31 g cm^{-3}. Data collection at 298 K out to 2θ = 50° provided 4645 reflections with $I > 3\sigma(I)$. Heavy atoms were located by the Patterson method and the remaining non-hydrogen atoms located by Fourier difference maps. The structure was refined by using 397 parameters to final R (R_w) values of 5.7% (6.4%).

(13) (a) *Tables of Interatomic Distances and Configuration in Molecules and Ions*; Sutton, L. E., Ed.; Specialist Publication No. 18; The Chemical Society: London, 1965; pp 53s, 513s. (b) Slater, J. C. *J. Chem. Phys.* **1964**, *41*, 3199.

(14) *Orbital Interactions in Chemistry*; Albright, T. A.; Burdett, J. K.; Whangbo, M.-H. Wiley-Interscience: New York, 1985; p 296.

(15) St. Denis, J. N.; Butler, W.; Glick, M. D.; Oliver, J. P. *J. Organomet. Chem.* **1977**, *129*, 1–16.